



Published in final edited form as:

Neuroimage. 2016 May 15; 132: 167–174. doi:10.1016/j.neuroimage.2016.02.028.

## Magnetic Susceptibility of Brain Iron is Associated with Childhood Spatial IQ

Kimberly L.H. Carpenter, PhD<sup>\*,1</sup>, Wei Li, PhD<sup>\*,2,3,4</sup>, Hongjiang Wei, PhD<sup>4</sup>, Bing Wu, PhD<sup>4,7</sup>, Xue Xiao<sup>4,8</sup>, Chunlei Liu, PhD<sup>4,5</sup>, Gordon Worley, MD<sup>6</sup>, and Helen Link Egger, MD<sup>1</sup>

<sup>1</sup>Department of Psychiatry and Behavioral Sciences, Duke University School of Medicine, Durham, North Carolina

<sup>2</sup>Research Imaging Institute, University of Texas Health Science Center, San Antonio, Texas

<sup>3</sup>Department of Ophthalmology, University of Texas Health Science Center, San Antonio, Texas

<sup>4</sup>Brain Imaging and Analysis Center, Duke University School of Medicine, Durham, North Carolina

<sup>5</sup>Department of Radiology, Duke University School of Medicine, Durham, North Carolina

<sup>6</sup>Department of Pediatrics, Program in Neurodevelopmental Disabilities, Division of Pediatric Neurology, Duke University School of Medicine, Durham, NC

<sup>7</sup>GE Healthcare, Beijing, China

<sup>8</sup>Department of Biomedical Engineering, Tsinghua University, Beijing, China

### Abstract

Iron is an essential micronutrient for healthy brain function and development. Because of the importance of iron in the brain, iron deficiency results in widespread and lasting effects on behavior and cognition. We measured iron in the basal ganglia of young children using a novel MRI method, quantitative susceptibility mapping, and examined the association of brain iron with age and cognitive performance. Participants were a community sample of 39 young children recruited from pediatric primary care who were participating in a five-year longitudinal study of child brain development and anxiety disorders. The children were ages 7 to 11 years old (mean age: 9.5 years old) at the time of the quantitative susceptibility mapping scan. The Differential Abilities Scale was administered when the children were 6 years old to provide a measure of general intelligence and verbal (receptive and expressive), non-verbal, and spatial performance. Magnetic susceptibility values, which are linearly related to iron concentration in iron-rich areas, were extracted from regions of interest within iron-rich deep gray matter nuclei from the basal ganglia, including the caudate, putamen, substantia nigra, globus pallidus, and thalamus. Controlling for scan age, there was a significant positive association between iron in the basal

**Corresponding Author:** Kimberly Carpenter (kimberly.carpenter@dm.duke.edu), Center for Developmental Epidemiology, Duke University Medical Center, Department of Psychiatry and Behavioral Sciences, Box 3454, Durham NC 27710, Phone: (919) 687-4686; Fax: (919) 687-4737.

<sup>\*</sup>Drs. Carpenter and Li contributed equally as primary authors on this work.

**Publisher's Disclaimer:** This is a PDF file of an unedited manuscript that has been accepted for publication. As a service to our customers we are providing this early version of the manuscript. The manuscript will undergo copyediting, typesetting, and review of the resulting proof before it is published in its final citable form. Please note that during the production process errors may be discovered which could affect the content, and all legal disclaimers that apply to the journal pertain.

ganglia and spatial IQ, with this effect being driven by iron in the right caudate. We also replicated previous findings of a significant positive association between iron in the bilateral basal ganglia and age. Our finding of a positive association between spatial IQ and mean iron in the basal ganglia, and in the caudate specifically, suggests that iron content in specific regions of the iron-rich deep nuclei of the basal ganglia influences spatial intelligence. This provides a potential neurobiological mechanism linking deficits in spatial abilities reported in children who were severely iron deficient as infants to decreased iron within the caudate.

## Keywords

Brain Iron; Quantitative Susceptibility Mapping; Spatial Intelligence; Caudate

## 1. Introduction<sup>1</sup>

Iron is an essential micronutrient for healthy brain function and development (Beard and Connor, 2003; Lozoff, 2007; Lozoff and Georgieff, 2006). Iron-containing enzymes and iron-dependent proteins are involved in dendrite and synapse development and iron-uptake in oligodendrocytes is essential for proper white matter myelination. Iron is also essential for the metabolism and catabolism of neurotransmitters, including dopamine, norepinephrine, serotonin, and GABA (Beard and Connor, 2003; Lozoff, 2007; Lozoff and Georgieff, 2006). Iron deficiency during infancy results in widespread and persistent effects on many neurophysiologic and regulatory processes, including cognitive, motor, and social-emotional behavior, suggesting that a lack of iron during neurodevelopment has lasting implications for brain function (Beard and Connor, 2003; Lozoff, 2007, 2011; Lozoff and Georgieff, 2006; Sachdev, 1993). Studies of iron deficiency in later childhood and adulthood have demonstrated similar negative consequences of iron deficiency (Beard and Connor, 2003; Sachdev, 1993), although iron repletion can, at least partially, reverse these negative effects (Khedr et al., 2008; Sachdev, 1993). To date, most studies linking iron deficiency to cognitive deficits in children have relied on peripheral measures of iron, which may be poorly correlated with iron in the brain (Li et al.). Furthermore, because nutritional iron is preferentially targeted towards maintaining hemoglobin concentration when iron levels are low, iron in the brain may reach critically low levels that have lasting impact on brain development well before blood samples reflect this critical shortage (Rao and Georgieff, 2002). Thus, in order to understand the neurobiological basis of the cognitive deficits resulting from iron deficiency, we must first explore the relationship between iron measured directly in the brain and the cognitive functions impacted by low iron levels. The current study aims to understand the neurobiological role of brain iron in children's cognitive functioning.

During the process of brain development, iron accumulates at variable rates in different anatomical locations, with the basal ganglia nuclei, including the caudate, putamen, substantia nigra, and the globus pallidus, having higher iron contents than the surrounding

<sup>1</sup>Abbreviations: Quantitative Susceptibility Mapping (QSM), Gradient Echo (GRE), Learning About the Developing Brain Study (LADB), Differential Abilities Scale (DAS), Multi-Echo Spoiled Gradient-Echo Sequence (ME-SPGR), Variable-filter-radius SHARP (V-SHARP), Regions of Interest (ROIs)

tissues (Hallgren and Sourander, 1958; Li et al., 2014; Li et al., 2011). Animal studies have demonstrated that iron deficiency during early brain development leads to alterations in the neurotransmitter systems of the basal ganglia, including decreased expression of dopaminergic receptors and decreased functioning of both dopaminergic and serotonergic transporters (Beard, 2001; Beard and Connor, 2003; Lozoff, 2007; Lozoff and Georgieff, 2006; Munoz and Humeres, 2012). Furthermore, neonatal iron deficiency results in global hypomyelination, including in the pathways connecting the iron-rich basal ganglia to the rest of the brain (Beard and Connor, 2003; Lozoff, 2007; Lozoff and Georgieff, 2006).

Many of the cognitive and behavioral functions implicated in iron deficiency including learning, memory, verbal and non-verbal reasoning, and visual-spatial abilities, rely on a prefrontal-subcortical dopaminergic network that includes the iron rich basal ganglia (Brown et al., 1997; Burgaleta et al., 2014; Khedr et al., 2008; Lozoff, 2007; Lozoff and Georgieff, 2006; Lozoff et al., 2000; MacDonald et al., 2014; Munoz and Humeres, 2012). The caudate and putamen, collectively referred to as the striatum, are the primary points of input for the basal ganglia, receiving projections from all parts of the cortex (Alexander et al., 1986; Grahn et al., 2008; Ring and Serra-Mestres, 2002). The striatum is then reciprocally connected to the substantia nigra through the nigrostriatal tract and sends outputs to both the substantia nigra and the globus pallidus, which then projects information back to the cortex through cortico-striatal loops (Alexander et al., 1986; Grahn et al., 2008). Both animal models and studies of humans with early life iron deficiency reveal cognitive deficits in line with disruption of prefrontal-basal ganglia pathways, suggesting that iron in the basal ganglia may influence cognitive functioning (Lozoff, 2011; Lozoff and Georgieff, 2006; Lukowski et al., 2010).

In this study, we measured brain iron in the basal ganglia of young children using quantitative susceptibility mapping (QSM), which is a novel MRI technique that is highly sensitive to paramagnetic non-heme iron in brain tissue and is linearly proportional to iron contents in certain brain areas (Schweser et al., 2011; Wharton et al., 2010; Wu et al., 2012b). It is well known that pediatric brains have much lower iron concentration than the adult brains in the deep brain nuclei regions (Aquino et al., 2009; Hallgren and Sourander, 1958), thus the development of sensitive method or non-invasive assessment of iron deposition is of particular importance in comparison to adult brain imaging studies. While the  $R2^*$  and  $R2'$  from gradient echo (GRE) MRI have long been used as a quantitative measure of brain iron (Aquino et al., 2009; Haacke et al., 2005), it was increasingly recognized that the GRE phase might provide more sensitivity to the iron deposition (Haacke et al., 2005). However, the GRE signal phase is not quantitative, since it is affected by surrounding tissue magnetic susceptibility distributions and the orientation. To overcome this problem, QSM was developed to deconvolve the phase using the magnetic dipole kernels to convert the nonlocal phase into magnetic susceptibility, (de Rochefort et al., 2010; Li et al., 2011; Liu et al., 2009; Schweser et al., 2011; Shmueli et al., 2009; Wharton et al., 2010; Wu et al., 2012a). The resultant tissue magnetic susceptibility inherits the high contrast of GRE signal phase, and provides clear contrast between the iron rich brain nuclei and the surrounding tissues. Magnetic susceptibility is a localized intrinsic property of tissue, and is typically not affected by the blooming artifact. As a result, the contrast and boundary of iron rich deep brain gray matter nuclei is often better delineated by QSM than

GRE magnitude  $R2'$  and  $R2^*$  (Lim et al., 2013). Furthermore, similar to  $R2^*$  ( $1/T2^*$ ), converging evidence suggests that magnetic susceptibility of iron rich gray matter is linearly proportional to the iron content (Bilgic et al., 2012; Langkammer et al., 2012; Schweser et al., 2011; Shmueli et al., 2009; Wu et al., 2012a). Given the excellent contrast and the linearity with iron, QSM is a promising candidate for noninvasive assessment of iron deposition in deep brain nuclei.

Using QSM, we explored, for the first time in children, the relationship between iron content measured directly in the brain and cognitive capabilities, as a step toward understanding the pathophysiology of iron deficiency and developmental sequelae. Although the current study only focuses on a subset of cognitive abilities, it is likely that other domains of behavior are also related to iron in the brain. Based on the literature linking iron deficiency to poor neurocognitive outcomes in children, we hypothesized that there would be an inverse relationship between iron in the basal ganglia and cognitive scores.

## 2. Material and Methods

### 2.1. Study Design & Participants

The Duke University Medical Center Institutional Review Board approved this study. Verbal assent from the child and written informed consent from the parent was obtained following a complete description of the study.

Participants were a convenience sample recruited from the Learning About the Developing Brain (LADB) study, a 5 year longitudinal study of child brain development and anxiety disorders. 102 children completed at least one MRI during the course of the Learning About the Developing Brain (LADB) study. A subset of 41 of these 102 children participated in the current pilot study of brain iron in childhood. Children were eligible for this pilot study if they had successfully completed at least 2 prior MRI scans as part of the larger LADB study. Given the pilot nature of this study, this enabled us to ensure the greatest chance of success at acquiring usable data. Additionally, only children who had a cognitive assessment when they were 6 years old were eligible for this study. The mean (standard deviation) time between the DAS assessment and the MRI was 2.74 (0.9) years.

Table 1 summarizes the demographic characteristics of the 39 children, ages 7 to 11, included in the pilot MRI study who had usable data. We discarded data from two children because of excess motion during the scan. Children in the pilot study were similar to the full sample of children from the LADB study who completed a cognitive assessment ( $N=183$ ) on race, sex, handedness, and overall, verbal, non-verbal, and spatial IQ (all  $p>0.35$ ).

### 2.2. Cognitive Assessment

The Differential Abilities Scale (DAS; Elliott, 1997) was administered when children were, on average, 6 years old. The DAS is a comprehensive, individually administered, clinical instrument for assessing cognitive abilities in children from ages 2 years 6 months through 17 years 11 months. The DAS provides a measure of overall general intelligence, as well as cluster scores for verbal abilities, non-verbal reasoning, and spatial abilities. The verbal abilities cluster score is a measure of a child's expressive and receptive verbal knowledge

and comprehension. The non-verbal reasoning cluster score is a measure of a child's inductive, sequential, and quantitative reasoning. The spatial abilities cluster score is a measure of a child's spatial visualization abilities, short-term visual recall, and perception of spatial orientation. All scores are reported as age-based standard scores ( $M = 100$ ,  $SD = 15$ ). In our sample, 28 children received an early years version of the DAS, which is given to children ages 2 years 6 months to 6 years 11 months, and 11 children received the school-age version, which is given to children 7 years and older.

### 2.3. Brain MRI

Each participant was scanned on a GE 3T MR750 scanner with an 8-channel receiver array coil at the Brain Imaging and Analysis Center at Duke University. A 3D multi-echo spoiled gradient-echo sequence (ME-SPGR) was used for quantitative susceptibility mapping. The scan parameters were: flip angle =  $20^\circ$ , TE of first echo = 5 ms, echo spacing = 2.94 ms, 8 echoes, TR = 55 ms, matrix =  $320 \times 320 \times 74$ , resolution =  $0.6 \times 0.6 \times 1.5 \text{ mm}^3$ , and there was no inversion time.

To determine the nonlinear transformation matrix between the individual participant space and the standard space, T1-weighted images of the same participants were acquired using a 3D IR prepared sequence similar to MPRAGE. The images were acquired in the sagittal view with the following parameters: data matrix =  $256 \times 256 \times 166$ , 1 mm isotropic resolution, flip angle =  $12^\circ$ , TE = 3.18 ms, TI = 450ms, and TR = 8.096 ms.

### 2.4. Quantitative Susceptibility Mapping (QSM)

Figure 1 and Supplementary Figure 1 depict the analysis pipeline for this study. QSM was performed using the STI Suite software package (Duke University) as described previously (Li et al., 2014; Li et al., 2011). Briefly, the brain was extracted from the magnitude using the brain extraction tool in FSL (Smith, 2002). For each echo, the phase was calculated from the summed coil-phase removed complex data, and then unwrapped using a Laplacian-based method (Li et al., 2011). The unwrapped phase maps from all coils were summed and normalized by the summation of the echo times to yield the frequency shift. The background frequency was removed using a variable-filter-radius SHARP (V-SHARP) method (Li et al., 2014; Schweser et al., 2011). Specifically, the diameter of the spherical mean filter decreases from a maximum value of 25 mm towards 1 mm at the brain boundary (Li et al., 2011; Wu et al., 2012b). Susceptibility maps were then derived from the brain tissue frequency shift using the LSQR method (Li et al., 2011).

### 2.5. Regions of Interest

The largest iron stores are within the deep gray matter nuclei of the brain, which include the basal ganglia. The current study focused on the putamen, globus pallidus, caudate nuclei, pulvinar nucleus of the thalamus, and the substantia nigra because of the higher levels of iron deposition in these regions, as compared to other brain regions (Hallgren and Sourander, 1958; Li et al., 2014; Li et al., 2011), as well as the role of the basal ganglia in cognitive functioning (Brown et al., 1997; Burgaleta et al., 2014; MacDonald et al., 2014). These regions of interest (ROIs) were obtained by warping a customized common atlas created in the standard space to each individual participant space using FSL (FMRIB,

University of Oxford, UK). A schematic diagram describing this procedure is shown in Figure 1 and Supplementary Figure 1. Briefly, the T1-weighted images were registered to a standard pediatric template developed from a sample of children ages 7 to 11 years old (Fonov et al., 2011) using FNIRT. The resulting registration matrices were used to wrap the susceptibility maps to the standard space and then averaged to generate mean susceptibility. We created the atlas for the deep gray matter nuclei based on the structural boundaries shown in the mean susceptibility images. As depicted in the representative images in panels A and B of Figure 2, QSM has good contrast with clear structural boundaries for all of these nuclei in our pediatric population. This study-specific common atlas for deep gray matter nuclei was then warped to each individual participant space using FSL. The ROIs of each participant were visually examined by two independent readers who were blind to the demographic data and behavioral test scores of the participants. Minor manual refinement of the ROIs was made when necessary. Figure 2, panel C depicts the segmentation of the iron-rich deep gray matter nuclei in a representative participant using the above approach. The susceptibility values by these two readers were modeled separately as repeated measures in all statistical analysis.

## 2.6. Data Analysis

Susceptibility values (X) were converted to iron (Fe) concentration with the following equation:  $X = 0.00089 \text{ ppm} * \text{Fe} - 0.022 \text{ ppm}$  (Langkammer et al., 2012). A measure of overall iron in the basal ganglia was computed by taking the average iron content across the ROIs. All statistical analyses were performed using mixed multiple regression models in SAS version 9.2 (SAS Institute Inc., Cary, NC). We ran three levels of models. Our first level of analysis involved fitting zero-order models, in which the relationship between brain iron and each of the primary demographics variables (i.e. age, sex, race, and handedness) were tested individually. The purpose of this set of analyses was to determine what, if any, of these demographic variables should be accounted for in our primary models. Of these demographic variables, only age was related to brain iron in our sample. As such, we included scan age as a covariate in all of our primary models, in which brain iron was the outcome and each individual IQ score (i.e. overall, verbal, non-verbal, and spatial – all modeled individually) was the predictor. Because the ROIs of each participant were visually examined by two independent readers, rater was included as a repeated measure and the standard errors and test statistics of fixed-effect parameters were adjusted using the empirical option.

We also performed three separate secondary analyses to ensure that other variables did not account for our findings. In the first set of secondary analyses, we explored whether there was a relationship between the clusters of cognitive abilities (verbal, non-verbal, and spatial) and the age of the child when they completed the DAS, which governed which version of the DAS they received, as well as the age of the child at the time of the QSM scan. In the second set of secondary analyses, we added anxiety as a covariate in all of the primary models (i.e. modeled age, IQ, and anxiety status with brain iron in each of the regions of interest as the outcome measures). In the third set of secondary analyses, we included caudate volume as a covariate in the model exploring the relationship between spatial IQ and iron in the caudate (i.e. modeled age, IQ, and caudate volume with iron in the caudate as the outcome measure).



### 3. Results

No association between iron in the basal ganglia and sex, race, or handedness existed in our sample (Supplementary Table 1). There was a significant positive association between iron in the basal ganglia and age ( $p<0.0001$ ), with the globus pallidus and the substantia nigra driving this significant association (Supplementary Table 1). Because of this significant association, we controlled for the effect of age in all subsequent analyses. By including age at scan as a covariate, we also account for the variable time between DAS assessment and the QSM scan.

Table 2 and Figure 3 summarize our IQ analyses. When controlling for scan age, iron in the basal ganglia was not significantly associated with overall IQ. There were also no statistically significant associations between iron in the basal ganglia and scores on verbal or non-verbal IQ subtests. However, there was a significant positive association between mean iron in the basal ganglia and spatial IQ ( $p=0.02$ ). We next examined whether there were specific regions within the basal ganglia associated with spatial IQ. Controlling for scan age, iron in the bilateral caudate (Right caudate:  $p<0.01$ ; Left caudate:  $p<0.05$ ) and the bilateral substantia nigra (Both  $p<0.05$ ) had a significant positive association with spatial IQ, however only the relationship with the right caudate survived FDR correction for multiple comparisons (FDR-adjusted  $p=0.04$ ). There was no association between spatial IQ and iron in the globus pallidus, putamen, or the pulvinar nucleus of the thalamus.

In addition to our primary analyses, we ran several secondary analyses to ensure that our findings could not be attributed to other variables in our study population. In the first of these analyses we sought to ensure that our findings were not due to an association between IQ and age at both the time of the DAS and at the time of the QSM scan. Neither age at DAS nor age at QSM scan were correlated with any of the IQ variables tested in this study (all  $p>0.4$ ). Scatter plots of the relationship between age at QSM scan and scores on each of the IQ sub-tests are included in Supplementary Figure 2. Additionally, to ensure that the relationship between iron in the right caudate and spatial IQ was not due to a difference in the size of the caudate, we ran a second analysis controlling for right caudate volume and the effect remained the same ( $p<0.01$ ). Finally, because the study population was drawn from a study of anxiety, we also ran all of our analyses controlling for anxiety and all of the regions that were significant in the original analyses remained significant and no new associations emerged as significant.

### 4. Discussion

In this study, we used a novel MRI technique, quantitative susceptibility mapping, to investigate the association between iron in the basal ganglia and cognitive functioning in a pediatric primary care sample of children ages 7 to 11 years old. QSM is highly sensitive to paramagnetic non-heme iron in brain tissue and the susceptibility values extracted from these scans can be converted to iron content (in mg/kg) through a simple linear equation (Langkammer et al., 2012; Schweser et al., 2011; Wharton et al., 2010; Wu et al., 2012b). Using this new imaging technology, we report, for the first time, that iron in the right caudate is associated with spatial IQ in school-age children.

Iron is an essential micronutrient for healthy brain function and development, having critical roles in neurodevelopmental processes (Beard and Connor, 2003; Lozoff, 2007; Lozoff and Georgieff, 2006). Animal research has demonstrated that iron deficiency in infancy is associated with long-term changes in myelination, synaptogenesis, and neurotransmitter functioning, particularly within dopaminergic system, with the greatest influence evident in the hippocampus, the substantia nigra, and the striatum (Beard and Han, 2009; Lozoff and Georgieff, 2006). In particular, iron deficiency has been linked to decreased expression of dopaminergic receptors in the striatum, which negatively influences functioning across the frontostriatal networks essential for cognition (Munoz and Hummeres, 2012). In humans, iron deficiency during infancy has been linked to long-term impairment in cognitive functions dependent on proper functioning of the dopaminergic basal ganglia pathways, namely visuospatial memory and selective recall for visual stimuli (Lozoff, 2007; Lozoff et al., 2000). Similar impairments, including decreased spatial IQ, have also been demonstrated in adults with iron deficiency (Khedr et al., 2008).

In the current study, we found that the iron content in the right caudate influences spatial IQ as measured with the DAS. Scores on the spatial ability cluster of the DAS reflect the ability to visualize spatial relationships, the perception of spatial orientations, analytical thinking abilities, and attention to visual detail (Elliott, 1997). Such visuospatial abilities have been shown to be foundational for success in Science, Technology, Engineering, and Math (STEM) fields (Wai et al., 2009). These skills have been linked to a neural network comprised of the lateral prefrontal cortex, caudate nucleus, palladium, substantia nigra, and the ventral anterior thalamic nucleus (Alexander et al., 1986; Brown et al., 1997; Burgaleta et al., 2014; Navas-Sanchez et al., 2014; Rhein et al., 2014). Furthermore, disruption of the dopaminergic systems underlying this network, as in the case of Parkinson's disease, is associated with decreased visuospatial function (Rhein et al., 2014; Ring and Serra-Mestres, 2002). This relationship is often right lateralized, with inherent asymmetry in the mesolimbic dopaminergic system and right hemisphere dominance for visuospatial processing (Molochnikov and Cohen, 2014).

To our knowledge, only two studies have investigated the association between brain iron and behavioral or cognitive outcomes in a pediatric population. The first reports an association between ADHD and decreases in peripheral ferritin levels and thalamic iron content (Cortese et al., 2012b). The second finds an association between decreased striatal and thalamic iron in medication-naïve ADHD patients, but not in treated patients, as compared to controls (Adisetiyo et al., 2014). These findings are consistent with previous studies linking peripheral ferritin levels to ADHD diagnosis (Cortese et al., 2012a) and provide some of the first evidence in humans linking differences in regional brain iron content to neuropsychiatric symptoms. Only twelve children met criteria for ADHD in the current study based on a structured parent interview with the Preschool Age Psychiatric Assessment (Egger et al., 2006). Given the relationship between ADHD and IQ (Frazier et al., 2004), it is possible that our relationship between lower iron in the basal ganglia and decreased spatial abilities is driven by differences in attentional abilities. Although attentional abilities are not measured in the DAS, we did explore whether there was a relationship between the ADHD diagnosis and iron in the basal ganglia and did not find any association. However, given that so few of the children met criteria for ADHD, it is not possible to determine if this was due



to a lack of statistical power to detect a real difference or a lack of an association between ADHD diagnosis and iron in the basal ganglia in our sample.

There are several strengths of our study. First, gray matter regional iron was measured through a novel MRI technique, QSM, which is highly sensitive to paramagnetic non-heme iron in brain tissue. Additionally, we achieved a high spatial resolution of  $0.6 \times 0.6 \times 1.5$ , providing us with millimeter resolution of the deep gray matter structures of interest. Achieving such a resolution required a protocol with a prolonged scan time of 21 min. Future studies could employ shortened imaging protocols using fast imaging methods, such as parallel imaging and compressed sensing, without significant degradation of image quality (Wu et al., 2012b; Wu et al., 2011). A final strength of our study was the investigation of brain iron in a non-clinical, normative sample of children from the community.

Our study also has limitations. First, despite some evidence for a poor correlation between peripheral iron and brain iron stores (Li et al.), it would have been valuable for us to have evaluated peripheral iron using serum tests for iron stores either at the time of the scan or in infancy. Second, too few subjects were studied to explore relationships between regional brain iron content and other plausible neuropsychological sequelae, including ADHD and other attentional processes. Additionally, many of our significant findings did not survive correction for multiple comparisons, which may be a result of our small sample size. It is difficult to know whether these findings would have been more robust with a larger sample size and therefore it is difficult to know whether other regions, namely the substantia nigra, are also contributing to the relationship between iron in the basal ganglia and spatial abilities. Third, two different forms of the DAS were used in our sample. While there is significant overlap between these two versions, we cannot be certain that they are identical. However, given that there was no correlation between IQ and the age of the child at both the time the QSM scan and their age when they completed the DAS, we are confident that the DAS form used did not impact our results. Furthermore, all of our primary analyses controlled for age at the time of the QSM scan, further accounting for any contribution of age to our findings. Lastly, there was approximately 2 years between when the DAS was completed and when the children were brought back for the QSM scan. As such, although there is some evidence that IQ remains relatively stable over the age range that we studied, (Moffitt et al., 1993), it is possible that the time-lapse represents a confound in our study as there is also evidence that IQ changes in a significant minority of children. Future studies should examine the correlation between iron in the brain and IQ when measured concurrently with the QSM scan.

There were also several limitations to our imaging protocol. Specifically, this study used an ROI-based approach, which assumes uniform iron distribution throughout any given gray matter structure. Previous studies have revealed an iron gradient within large gray matter nuclei, especially within the putamen and globus pallidus (Aquino et al., 2009; Li et al., 2014), future studies need to further investigate the association between iron contents and cognitive function using more advanced voxel-wise approaches. Additionally, QSM is not suitable for measuring the brain iron in white matter regions because of complication of magnetic susceptibility anisotropy due to the molecular anisotropy of myelin lipids (Li and

Liu, 2013; Li et al., 2012; Liu, 2010; Liu et al., 2012). Nevertheless, the susceptibility of iron rich gray matter is considered to be isotropic and demonstrated to be linearly correlated with the iron contents (Schweser et al., 2011; Wharton et al., 2010; Wu et al., 2012b). Furthermore, magnetic susceptibility values measured by QSM are relative as they are affected by several factors including RF frequency and image phase processing procedures. Identifying an absolute and universal reference remains an open question. In our study, no specific regions of the brain were chosen as reference, which essentially set the mean of the whole brain as the reference. Because the whole brain contains many contributors to magnetic susceptibility, it is less likely to be affected by variations in any single factor (Li et al., 2014). Finally, the literature supporting the relationship between susceptibility and iron is based on studies in adults (e.g. Langkammer et al., 2012) and have not been conducted in the age range considered in this study. Thus, without further post-mortem validation studies with larger age ranges, we cannot rule out that the QSM signal in our pediatric population is due to something other than a change in brain iron content.

## 5. Conclusions

In conclusion, our finding of a positive association between iron in the right caudate and spatial IQ suggests that iron in the caudate influences the ability to perceive, visualize, and remember spatial information. This provides preliminary support for the hypothesis proposed by Lozoff (2011) that disruption of dopaminergic systems, including the nigrostriatal and mesocortical pathways, may contribute to the cognitive deficits, in particular difficulties with visuospatial processing, associated with iron deficiency. Given the importance of these abilities for success, particularly in science, technology, engineering, and math (STEM) fields, it is critical that we begin identifying children who are at risk for low brain iron levels so that we can intervene before their brain development is irreversibly impacted. Understanding the mechanisms by which brain iron affects cognitive development in young children is a first step towards this, providing potential targets for interventions that go beyond iron supplementation and instead focus on the underlying neurobiological sequelae of early iron deficiency.

## Supplementary Material

Refer to Web version on PubMed Central for supplementary material.

## Acknowledgments

This study was funded by the Duke University Brain Imaging and Analysis Center Pilot Hours, an NIMH grant (R01-MH-081025) awarded to Dr. Egger, and supported in part by NIMH R01MH096979, NINDS R01NS079653 and National Multiple Sclerosis Society through grant RG4723 to Dr. Liu. The authors would like to thank Drs. William Copeland, Adrian Angold, E. Jane Costello, Lauren Franz, Gary Maslow, and Sherika Hill, all of Duke University, for their thoughtful feedback on this manuscript and many fruitful discussions concerning this data. The authors would like to thank our study coordinators, Kristen Caldwell and Brian Small, and our interviewing team: Alice Bartram, Carmen Bondy, Jason Chavarria, Adrienne Pearson, Kirsten Robb, Alex Vann, and Lucy Zhang. Finally, we are especially grateful to the families who participated in this study.

## References

- Adisetiyo V, Jensen JH, Tabesh A, Deardorff RL, Fieremans E, Di Martino A, Gray KM, Castellanos FX, Hupfel JA. Multimodal MR imaging of brain iron in attention deficit hyperactivity disorder: a noninvasive biomarker that responds to psychostimulant treatment? *Radiology*. 2014; 272:524–532. [PubMed: 24937545]
- Alexander GE, DeLong MR, Strick PL. Parallel organization of functionally segregated circuits linking basal ganglia and cortex. *Annu Rev Neurosci*. 1986; 9:357–381. [PubMed: 3085570]
- Aquino D, Bizzi A, Grisoli M, Garavaglia B, Bruzzone MG, Nardocci N, Savoirdo M, Chiapparini L. Age-related iron deposition in the basal ganglia: quantitative analysis in healthy subjects. *Radiology*. 2009; 252:165–172. [PubMed: 19561255]
- Beard J, Han O. Systemic iron status. *Biochim Biophys Acta*. 2009; 1790:584–588. [PubMed: 18930117]
- Beard JL. Iron biology in immune function, muscle metabolism and neuronal functioning. *J Nutr*. 2001; 131:568S–579S. discussion 580S. [PubMed: 11160590]
- Beard JL, Connor JR. Iron status and neural functioning. *Annu Rev Nutr*. 2003; 23:41–58. [PubMed: 12704220]
- Bilgic B, Pfefferbaum A, Rohlfing T, Sullivan EV, Adalsteinsson E. MRI estimates of brain iron concentration in normal aging using quantitative susceptibility mapping. *Neuroimage*. 2012; 59:2625–2635. [PubMed: 21925274]
- Brown LL, Schneider JS, Lidsky TI. Sensory and cognitive functions of the basal ganglia. *Curr Opin Neurobiol*. 1997; 7:157–163. [PubMed: 9142758]
- Burgaleta M, MacDonald PA, Martinez K, Roman FJ, Alvarez-Linera J, Ramos Gonzalez A, Karama S, Colom R. Subcortical regional morphology correlates with fluid and spatial intelligence. *Hum Brain Mapp*. 2014; 35:1957–1968. [PubMed: 23913782]
- Cortese S, Angriman M, Lecendreux M, Konofal E. Iron and attention deficit/hyperactivity disorder: What is the empirical evidence so far? A systematic review of the literature. *Expert Rev Neurother*. 2012a; 12:1227–1240. [PubMed: 23082739]
- Cortese S, Azoulay R, Castellanos FX, Chalard F, Lecendreux M, Chechin D, Delorme R, Sebag G, Sbarbati A, Mouren MC, Bernardina BD, Konofal E. Brain iron levels in attention-deficit/hyperactivity disorder: a pilot MRI study. *World J Biol Psychiatry*. 2012b; 13:223–231. [PubMed: 21585274]
- de Rochefort L, Liu T, Kressler B, Liu J, Spincemaille P, Lebon V, Wu J, Wang Y. Quantitative susceptibility map reconstruction from MR phase data using bayesian regularization: validation and application to brain imaging. *Magn Reson Med*. 2010; 63:194–206. [PubMed: 19953507]
- Egger HL, Erkanli A, Keeler G, Potts E, Walter BK, Angold A. Test-Retest Reliability of the Preschool Age Psychiatric Assessment (PAPA). *J Am Acad Child Adolesc Psychiatry*. 2006; 45:538–549. [PubMed: 16601400]
- Elliott, CD. *The Differential Ability Scales*. Guilford Press; New York: 1997.
- Fonov V, Evans AC, Botteron K, Almli CR, McKinstry RC, Collins DL. Unbiased average age-appropriate atlases for pediatric studies. *Neuroimage*. 2011; 54:313–327. [PubMed: 20656036]
- Frazier TW, Demaree HA, Youngstrom EA. Meta-Analysis of Intellectual and Neuropsychological Test Performance in Attention-Deficit/Hyperactivity Disorder. *Neuropsychology*. 2004; 18:543–555. [PubMed: 15291732]
- Grahn JA, Parkinson JA, Owen AM. The cognitive functions of the caudate nucleus. *Prog Neurobiol*. 2008; 86:141–155. [PubMed: 18824075]
- Haacke EM, Cheng NY, House MJ, Liu Q, Neelavalli J, Ogg RJ, Khan A, Ayaz M, Kirsch W, Obenaus A. Imaging iron stores in the brain using magnetic resonance imaging. *Magn Reson Imaging*. 2005; 23:1–25. [PubMed: 15733784]
- Hallgren B, Sourander P. The effect of age on the non-haemin iron in the human brain. *J Neurochem*. 1958; 3:41–51. [PubMed: 13611557]
- Khedr E, Hamed SA, Elbeih E, El-Shereef H, Ahmad Y, Ahmed S. Iron states and cognitive abilities in young adults: neuropsychological and neurophysiological assessment. *Eur Arch Psychiatry Clin Neurosci*. 2008; 258:489–496. [PubMed: 18574611]

- Langkammer C, Schweser F, Krebs N, Deistung A, Goessler W, Scheurer E, Sommer K, Reishofer G, Yen K, Fazekas F, Ropele S, Reichenbach JR. Quantitative susceptibility mapping (QSM) as a means to measure brain iron? A post mortem validation study. *Neuroimage*. 2012
- Li W, Langkammer C, Chou YH, Petrovic K, Schmidt R, Song AW, Madden DJ, Ropele S, Liu C. Association between increased magnetic susceptibility of deep gray matter nuclei and decreased motor function in healthy adults. *Neuroimage*. 2015; 105:45–52. [PubMed: 25315786]
- Li W, Liu C. Comparison of Magnetic Susceptibility Tensor and Diffusion Tensor of the Brain. *J Neurosci Neuroeng*. 2013; 2:431–440. [PubMed: 25401058]
- Li W, Wu B, Avram AV, Liu C. Magnetic susceptibility anisotropy of human brain in vivo and its molecular underpinnings. *Neuroimage*. 2012; 59:2088–2097. [PubMed: 22036681]
- Li W, Wu B, Batrachenko A, Bancroft-Wu V, Morey RA, Shashi V, Langkammer C, De Bellis MD, Ropele S, Song AW, Liu C. Differential developmental trajectories of magnetic susceptibility in human brain gray and white matter over the lifespan. *Hum Brain Mapp*. 2014; 35:2698–2713. [PubMed: 24038837]
- Li W, Wu B, Liu C. Quantitative susceptibility mapping of human brain reflects spatial variation in tissue composition. *Neuroimage*. 2011; 55:1645–1656. [PubMed: 21224002]
- Lim IAL, Faria AV, Li X, Hsu JTC, Airan RD, Mori S, van Zijl PCM. Human brain atlas for automated region of interest selection in quantitative susceptibility mapping: Application to determine iron content in deep gray matter structures. *Neuroimage*. 2013; 82:449–469. [PubMed: 23769915]
- Liu C. Susceptibility tensor imaging. *Magn Reson Med*. 2010; 63:1471–1477. [PubMed: 20512849]
- Liu C, Li W, Wu B, Jiang Y, Johnson GA. 3D fiber tractography with susceptibility tensor imaging. *Neuroimage*. 2012; 59:1290–1298. [PubMed: 21867759]
- Liu T, Spincemaille P, de Rochefort L, Kressler B, Wang Y. Calculation of susceptibility through multiple orientation sampling (COSMOS): A method for conditioning the inverse problem from measured magnetic field map to susceptibility source image in MRI. *Magnetic Resonance in Medicine*. 2009; 61:196–204. [PubMed: 19097205]
- Lozoff B. Iron deficiency and child development. *Food Nutr Bull*. 2007; 28:S560–571. [PubMed: 18297894]
- Lozoff B. Early iron deficiency has brain and behavior effects consistent with dopaminergic dysfunction. *J Nutr*. 2011; 141:740S–746S. [PubMed: 21346104]
- Lozoff B, Georgieff MK. Iron deficiency and brain development. *Semin Pediatr Neurol*. 2006; 13:158–165. [PubMed: 17101454]
- Lozoff B, Jimenez E, Hagen J, Mollen E, Wolf AW. Poorer behavioral and developmental outcome more than 10 years after treatment for iron deficiency in infancy. *Pediatrics*. 2000; 105:E51. [PubMed: 10742372]
- Lukowski AF, Koss M, Burden MJ, Jonides J, Nelson CA, Kaciroti N, Jimenez E, Lozoff B. Iron deficiency in infancy and neurocognitive functioning at 19 years: evidence of long-term deficits in executive function and recognition memory. *Nutr Neurosci*. 2010; 13:54–70. [PubMed: 20406573]
- MacDonald PA, Ganjavi H, Collins DL, Evans AC, Karama S. Investigating the relation between striatal volume and IQ. *Brain Imaging Behav*. 2014; 8:52–59. [PubMed: 23813349]
- Moffitt TE, Caspi A, Harkness AR, Silva PA. The natural history of change in intellectual performance: who changes? How much? Is it meaningful? *J Child Psychol Psychiatry*. 1993; 34:455–506. [PubMed: 8509490]
- Molochnikov I, Cohen D. Hemispheric differences in the mesostriatal dopaminergic system. *Frontiers in Systems Neuroscience*. 2014; 8:110. [PubMed: 24966817]
- Munoz P, Humeres A. Iron deficiency on neuronal function. *Biometals*. 2012; 25:825–835. [PubMed: 22639188]
- Navas-Sanchez FJ, Aleman-Gomez Y, Sanchez-Gonzalez J, Guzman-De-Villoria JA, Franco C, Robles O, Arango C, Desco M. White matter microstructure correlates of mathematical giftedness and intelligence quotient. *Hum Brain Mapp*. 2014; 35:2619–2631. [PubMed: 24038774]
- Rao R, Georgieff MK. Perinatal aspects of iron metabolism. *Acta Paediatr Suppl*. 2002; 91:124–129. [PubMed: 12477276]

- Rhein C, Muhle C, Richter-Schmidinger T, Alexopoulos P, Doerfler A, Kornhuber J. Neuroanatomical correlates of intelligence in healthy young adults: the role of basal ganglia volume. *PLoS One*. 2014; 9:e93623. [PubMed: 24699871]
- Ring HA, Serra-Mestres J. Neuropsychiatry of the basal ganglia. *J Neurol Neurosurg Psychiatry*. 2002; 72:12–21. [PubMed: 11784818]
- Sachdev P. The neuropsychiatry of brain iron. *J Neuropsychiatry Clin Neurosci*. 1993; 5:18–29. [PubMed: 8094018]
- Schweser F, Deistung A, Lehr BW, Reichenbach JR. Quantitative imaging of intrinsic magnetic tissue properties using MRI signal phase: an approach to in vivo brain iron metabolism? *Neuroimage*. 2011; 54:2789–2807. [PubMed: 21040794]
- Shmueli K, de Zwart JA, van Gelderen P, Li TQ, Dodd SJ, Duyn JH. Magnetic susceptibility mapping of brain tissue in vivo using MRI phase data. *Magnetic Resonance in Medicine*. 2009; 62:1510–1522. [PubMed: 19859937]
- Smith SM. Fast robust automated brain extraction. *Hum Brain Mapp*. 2002; 17:143–155. [PubMed: 12391568]
- Wai J, Lubinski D, Benbow CP. Spatial ability for STEM domains: Aligning over 50 years of cumulative psychological knowledge solidifies its importance. *Journal of Educational Psychology*. 2009; 101:817–835.
- Wharton S, Schafer A, Bowtell R. Susceptibility mapping in the human brain using threshold-based k-space division. *Magn Reson Med*. 2010; 63:1292–1304. [PubMed: 20432300]
- Wu B, Li W, Guidon A, Liu C. Whole brain susceptibility mapping using compressed sensing. *Mag Reson Med*. 2012a; 67:137–147.
- Wu B, Li W, Guidon A, Liu C. Whole brain susceptibility mapping using compressed sensing. *Magn Reson Med*. 2012b; 67:137–147. [PubMed: 21671269]
- Wu B, Li W, Liu C. Fast in vivo susceptibility imaging using compressed sensing and parallel imaging. *Acoustics, Speech and Signal Processing (ICASSP)*, 2014 IEEE International Conference on. 2011:4474.

**Highlights**

- We explore the relationship between brain iron, age, and cognition in children.
- Iron in the basal ganglia is positively associated with age.
- Iron in the basal ganglia is associated with spatial IQ in children.
- Iron in the right caudate drove this association.



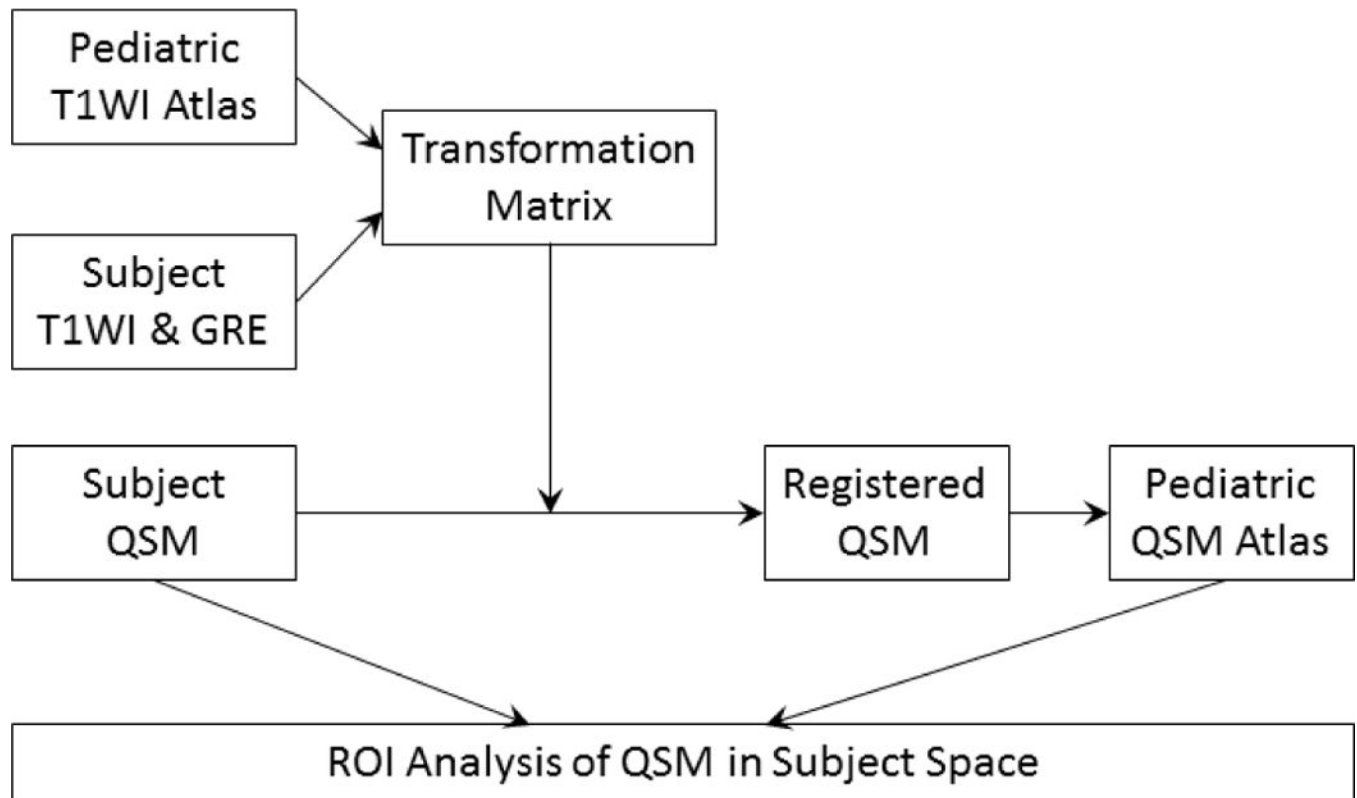


**Figure 1. Summary of ROI analysis pipeline**

T1-weighted images (T1WI) and GRE magnitude images (echo 1) were used to calculate the transformation matrix that maps the GRE images to a standard pediatric T1WI atlas. The resulting transformation matrix was then used to register individual subject's susceptibility map to the pediatric atlas. The registered QSM maps from all subjects were then averaged to form a pediatric QSM atlas. ROIs were first defined on the QSM atlas, then inverse transformed back to the individual subject space of the native QSM maps. Finally, the mean susceptibility of each ROI was calculated for each subject on which subsequent statistical analysis was performed. A more detailed flowchart of the pipeline can be found in Supplementary Figure 1.

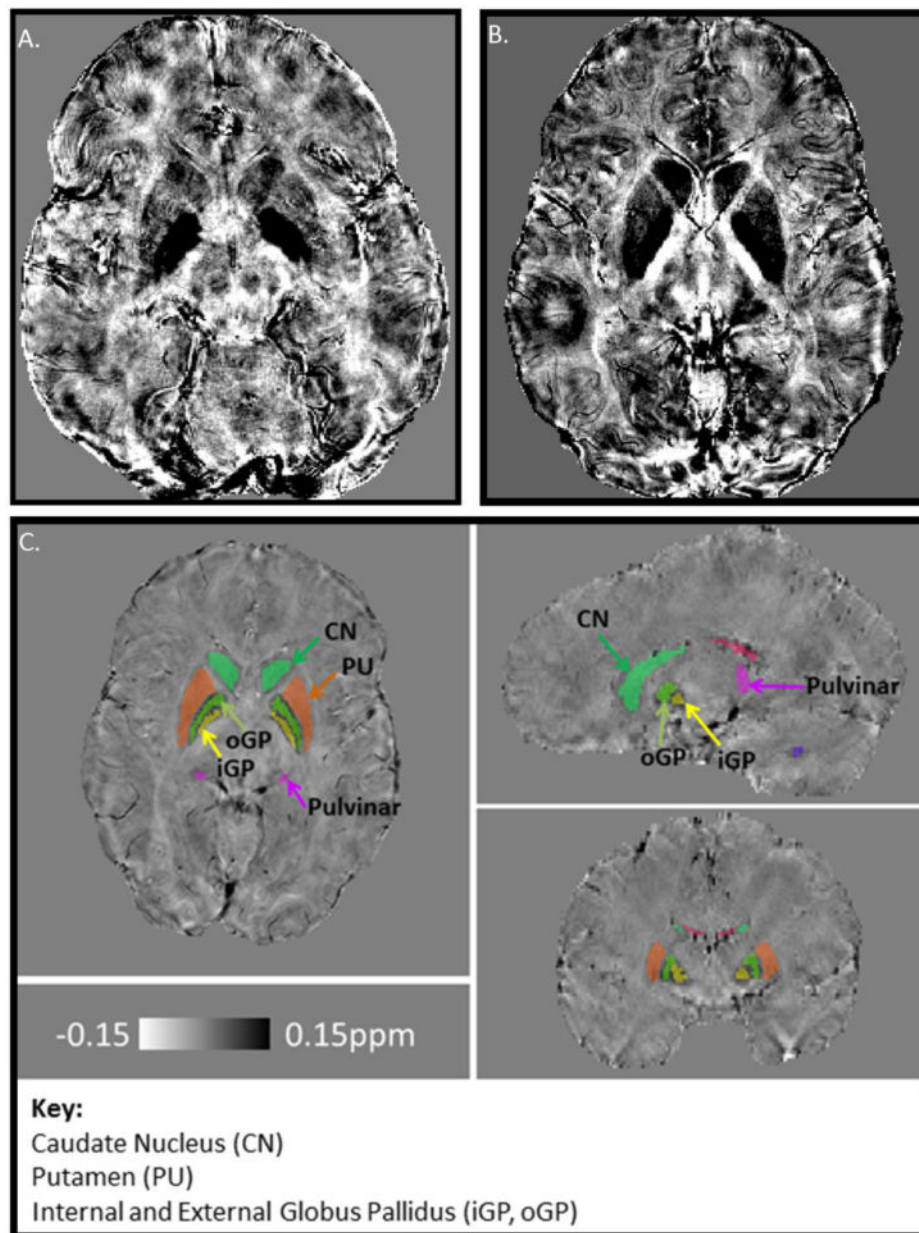


**Figure 2. Representative QSM Scans and Regions of Interest**

The top two panels depict representative QSM scans from an 8-year-old (panel A) and an 11-year-old (panel B). Panel C depicts the iron-rich nuclei within the deep gray matter that were selected as regions of interest.

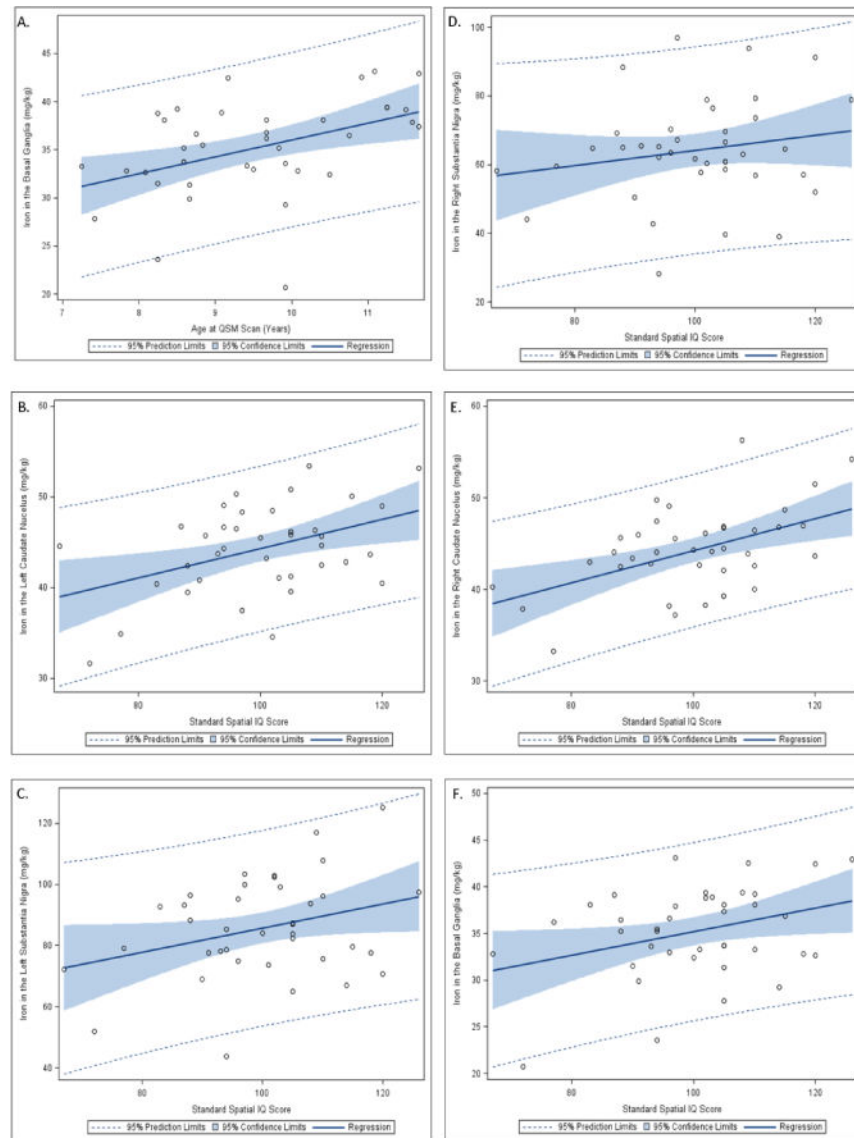


**Figure 3. Average iron in the basal ganglia and spatial IQ**

Scatter plots for the relationship between spatial IQ and age at QSM scan are depicted in panel A. Additional panels depict scatter plots of the relationship between spatial IQ and iron in the (B) Left Caudate ( $p < 0.05$ ), (C) Left Substantia Nigra ( $p < 0.05$ ), (D) Right Substantia Nigra ( $p < 0.05$ ), (E) Right Caudate ( $p < 0.01$ ), and (F) Basal Ganglia overall ( $p < 0.05$ ). See Table 2 for parameter estimates and standard deviations.

**Table 1**

## Sample Characteristics

	QSM Pilot (N=39)		Full Sample (N=183)	
Race				
African American	20		90	
Not African American	19		93	
Sex				
Female	22		100	
Male	17		83	
Right Handed	31		142	
	Mean [S.D.]	Range	Mean [S.D.]	Range
Age at Scan	9.51 [1.25]	7.25–11.67	–	–
Age at DAS	6.80 [0.71]	6.00–8.25	6.62 [0.54]	5.42–8.50
DAS IQ <sup>a</sup>				
Overall	100.64 [15.17]	61–130	100.02 [14.03]	48–138
Verbal	102.41 [13.80]	81–142	101.83 [13.75]	67–142
Non-Verbal	99.26 [16.14]	58–142	100.21 [14.18]	37–140
Spatial	99.69 [13.00]	67–126	98.08 [12.80]	58–142

<sup>a</sup>DAS = Differential Ability Scale

Results from primary models where brain iron in each region of interest was the outcome, individual IQ scores were the predictors, and age at scan was included as a covariate.

Table 2

IQ Measure (modeled Separately)	Iron (mg/kg) by Region of Interest in the Basal Ganglia									
	Right CN	Left CN	Right Gp	Left Gp	Right SN	Left SN	Right PU	Left PU	Right TH	Left TH
Overall IQ	0.11 [0.04]	0.07 [0.05]	-0.02 [0.07]	-0.02 [0.08]	0.19 [0.14]	0.21 [0.17]	-0.02 [0.03]	-0.05 [0.03]	-0.01 [0.05]	0.001 [0.07]
Verbal IQ	0.11 [0.05]	0.04 [0.05]	-0.08 [0.07]	-0.11 [0.08]	0.05 [0.15]	0.08 [0.19]	-0.09 [0.03]	-0.09 [0.03]	-0.01 [0.05]	0.08 [0.07]
Non-Verbal IQ	0.06 [0.04]	0.04 [0.03]	-0.02 [0.07]	-0.03 [0.07]	0.16 [0.13]	0.12 [0.16]	0.005 [0.03]	-0.02 [0.03]	-0.04 [0.06]	-0.05 [0.07]
Spatial IQ	0.16† [0.05]	0.13 [0.05]	0.06 [0.10]	0.10 [0.08]	0.32 [0.16]	0.40 [0.18]	0.03 [0.04]	-0.03 [0.04]	0.04 [0.05]	-0.004 [0.08]

**Note:** Values represent model corrected parameter estimates [standard deviation]. We modeled each region of interest (N=10) and each IQ Measure (N=4) separately, for a total of 40 individual models. As such, we controlled for multiple comparisons with FDR-correction. Significance is identified as follows: †FDR-Corrected p<0.05.

**Key:** Basal Ganglia=BG, Caudate=CN, Globus Pallidus=GP, Substantia Nigra=SN, Putamen=PU, Pulvinar Nucleus of the Thalamus=TH